Hindawi
Advances in Civil Engineering
Volume 2019, Article ID 3105017, 10 pages
https://doi.org/10.1155/2019/3105017

Research Article

Dynamic Damage Mechanism of Coal Wall in Deep Longwall Face

Shuaifeng Lu,[1,2] **Sifei Liu**,[1,2] **Zhijun Wan**,[1,2] **Jingyi Cheng**,[1,2] **Zhuangzhuang Yang**,[1,2] **and Peng Shi**[1,2]

[1]*Key Laboratory of Deep Coal Resource Mining (CUMT), Ministry of Education of China, Xuzhou 221116, China*
[2]*School of Mines, China University of Mining and Technology, Xuzhou 221116, China*

Correspondence should be addressed to Zhijun Wan; zhjwan@cumt.edu.cn

Received 15 August 2019; Revised 14 November 2019; Accepted 29 November 2019; Published 14 December 2019

Academic Editor: Farhad Aslani

The stability of coal wall in deep longwall face has always been a research hotspot. In this study, pure vibration signals in the coal wall during the operation of mining machinery were obtained for the first time, and their energy is mainly concentrated in 7–12 Hz. Besides, based on the law of stress wave propagation, with the coal wall of deep longwall taken as the research object, the theory of dynamic damage in coal wall was put forward from the perspective of dynamics. The results show that the loading and unloading waves generated by the mining machinery disturbance will be reflected and transmitted at the interface with different impedances, resulting in the formation of multiple unloading and loading waves and multiple tensile stress zones and stress concentration zones. These stress concentration zones tend to induce tensile stress generation and coal failure. As a result, the coal undergoes zonal failure and spalling. Through the vibration test of coal, it is found that the crack development of the coal sample can be divided into five stages, and the phenomena of zonal failure and spalling occur, which is consistent with the theory. At the same time, the sample that has gone through a large disturbance cannot be further damaged by a small disturbance, which is verified by the damage statistical constitutive model based on the isotropy hypothesis.

1. Introduction

Fully mechanized mining technology, which has been widely used in deep mines in China, is considered as a production mode to achieve efficient production and improve recovery rate [1–3]. The factors affecting coal wall stability in the working face have been extensively researched on, and these researches mainly focused on the coal seam, the mining height, the roof load, and the mechanical properties of coal and rock [4–6]. Theoretical modeling on coal wall stability has also been carried out by researchers. These models include the shaft theory [7, 8], the Ritz method [9], and the shear model [10], all of which belong to static analysis. In fact, when coal seam mining reaches a certain depth, the effect of dynamic disturbance becomes more significant. Therefore, it is necessary to strengthen the analysis on the influence of dynamic disturbance on coal wall stability in deep wells.

As shown in Figure 1 [11], the force sources at the coal wall of working face in a deep well include the following: the static load stress σ_s caused by stress adjustment and the dynamic load stress σ_d caused by mechanical disturbance of working face. In the area near the working face, the static load stress is higher while the ultimate strength of coal is lower. When the dynamic load is superimposed on the working face area and exceeds the ultimate strength of coal, the coal will be damaged, and even sudden disasters like rock burst will occur. The dynamic load stress at the working face mainly includes vibration disturbance caused by mining machinery and coal burst induced by mining. Many researchers have studied dynamic load disturbance. Cheng et al. studied the mechanical characteristics of siltstone under high static load and frequent dynamic load disturbance [12]. You et al. analyzed the correlation between elastic energy index and damage evolution through the optimized triaxial cyclic loading and unloading tests [13]. Badge and Petroš concluded that the frequency and amplitude of dynamic load disturbance would affect the strength and capacity of rock [14]. Hargraves and Upfold [15] believed that the disturbance waves generated tensile

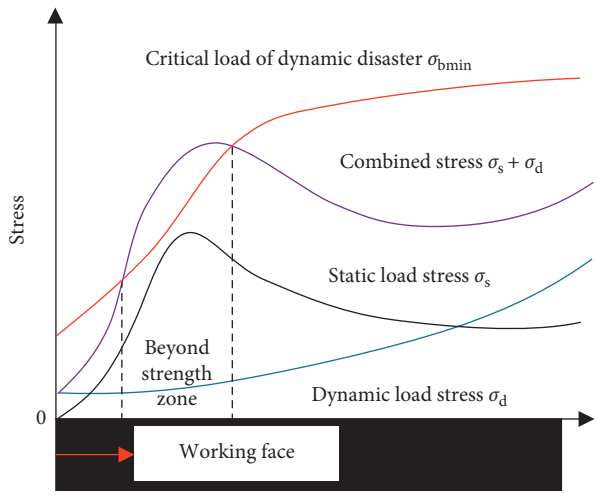

Figure 1: Superposition of loads near coal working faces.

stress when propagating in coal and rock mass and tensile failure was the primary form of failure. Li et al. studied the effects of cyclic loading and unloading on the permeability of broken coal [16]. The results showed that as the cyclic loading and unloading time went by, the permeability loss, stress sensitivity, and crushing amount of broken coal were gradually reduced. In their researches on vibration-induced failure of coal and rock mass, Litwiniszyn [17] and Pan et el. [18] revealed that vibration would promote the evolution of coal fractures and reduce the strength of coal. Zhan and Qi studied the dynamic response of the SV wave to the horizontal layered-structure rock slope, and the results revealed that slope structure played a dominant role in the stability of rock slope under dynamic load [19]. Li et al. found that in the process of vibration wave propagation, compressive stress and tensile stress often appeared alternately, which could induce strong vibration, damage, or even damage of coal and rock mass [20–22]. Li et al. also discussed the dynamic response characteristics and damage mechanism of coal and rock mass under the longitudinal wave mode [23].

To investigate the influence of mining machinery disturbance on the coal wall in deep wells and discuss the mechanism of dynamic damage in the coal wall, following work was conducted in the study. First, vibration signals generated in the coal wall during the operation of coal mining machinery were collected. Then, the process of vibration wave propagation in coal was analyzed in light of the rule of stress wave propagation. Moreover, the mechanism of dynamic damage of coal wall was proposed and verified by an experiment. Finally, the stress evolution law and fracture development process of coal were analyzed by using the damage statistical constitutive model based on the isotropy assumption.

2. Vibration Signals Generated during the Operation of Mining Machinery

Scholars [24] tried to acquire the signals of disturbance caused by coal mining machinery operation in the coal wall. However, these disturbance signals can hardly be accurately acquired even after a variety of noise processing due to the great influence of roof rupture on signal acquisition in the mining process. In this study, with the aid of the fully mechanized mining face of the State Energy Excavating Equipment R&D Testing Center, the dynamic disturbance caused by coal mining machinery operation in the coal wall was acquired in the laboratory, and the influence of other dynamic disturbances was avoided. The pure-disturbance signals caused by the mechanical equipment operation in the coal wall were obtained for the first time. In addition, given the fact that the study mainly aims to investigate the influence of dynamic disturbance of coal mining machinery on the coal wall, the effect of roof on coal wall crushing can be ignored in the experimental process.

2.1. Experimental System. The State Energy Excavating Equipment R&D Testing Center is the world's largest comprehensive excavating equipment testing laboratory that boasts the most advanced testing methods and the most complete functions. The 70 meter-long and 3 meter-high simulated fully mechanized coal face takes coal as the aggregate, and its properties such as joint, hardness, toughness, dust, crack, and collapse are the most similar to those of real coal wall in the world. The details are shown in Figure 2. The TDS microseismic monitoring system, which is composed of a main station and a substation, forms an observation network through wireless means. The sampling frequency is 1 kHz.

2.2. Experimental Scheme. The influence of vibration on the stability of coal not only depends on the energy and form of the excitation source but also is closely related to some inherent characteristics of the coal, especially the parameters like natural vibration frequency [25]. Therefore, the natural vibration characteristics of coal wall were acquired first, after which the vibration characteristics of coal wall under the action of coal cutting were acquired. Specific operation steps are as follows: first, the acquisition system was arranged in the simulated working face without any disturbance to acquire the vibration characteristics of coal wall. Then, the vibration characteristics of coal wall under straight cutting and oblique (S-shape) cutting conditions were recorded, respectively.

2.3. HHT Analysis of Coal Wall Vibration Signal. In this paper, the 10 second vibration signals of Substation #1 were selected for Hilbert–Huang analysis [26, 27] (Figure 3). As a whole, the signals are divided into the frequency band I (0–12 Hz) and the frequency band II (12–27 Hz). Besides, the signals are mainly concentrated in the low-frequency band of 7–12 Hz. The disturbance signals and natural vibration signals are prone to resonance as they share similar frequencies. In frequency band I, natural vibration signals do not exhibit obvious carrier characteristics, while the coal cutting signals show the characteristics of low main frequency and large amplitude, indicating that the mechanical work forces the coal to vibrate within a relatively large range.

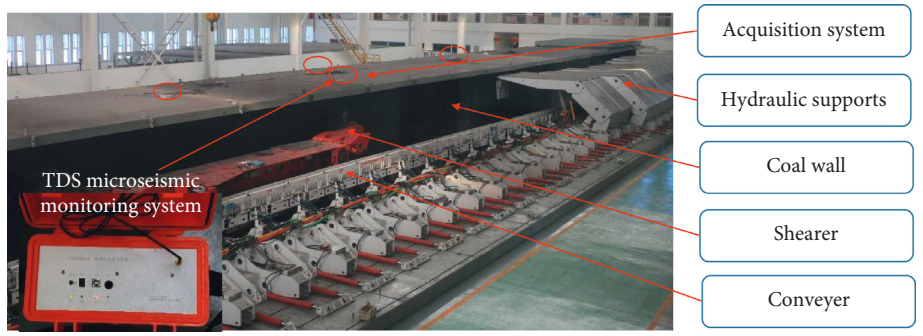

Figure 2: Comprehensive excavating equipment testing lab and acquisition system.

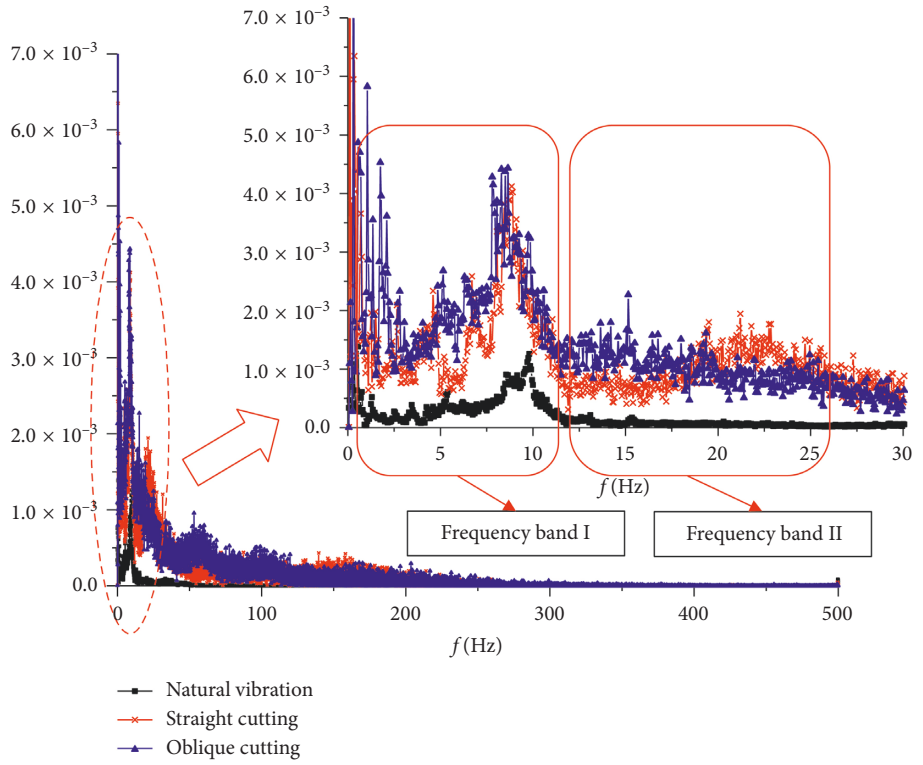

Figure 3: Hilbert spectrum of the vibration signal.

In frequency band II, the intensity of oblique cutting signals is higher than that of straight coal cutting signals in the 12–18 Hz segment; on the contrary, in the 18–27 Hz segment, different coal cutting methods display different disturbance characteristics. Therefore, the frequency of coal wall vibration signals approximates 10 Hz. Since the data acquired by the microseismic system are acceleration data, the displacement value (3.72 mm at most) of the vibration is obtained by integrating it within a period. A coal seam with a height of 3 m can be considered to have experienced a strain disturbance of 1.2‰.

3. Dynamic Damage Mechanism

3.1. Model. Plastic damage will occur in the coal wall under the action of advanced abutment pressure, and an elastic-plastic interface will be formed. As shown in Figure 4, Areas A and B are the elastic area and the plastic area, respectively. According to the law of stress wave propagation, the wave impedance of the plastic coal in front of the working face is smaller than that of the elastic coal, so the stress wave is refracted and reflected in the elastic-plastic interface.

Since the operation of coal mining machinery just generates limited disturbance energy in the working face and affects a small range of area, this study focuses on analyzing the effect of disturbance load on Area A. In order to study and analyze the law of dynamic response of elastic-plastic composite coal under disturbance load, the following assumptions are made:

(1) The average wave velocities in the plastic and elastic areas are c_l and c_e, respectively.

(2) Stress and velocity of interfacial coal particles are consistently distributed. That is, the velocity and

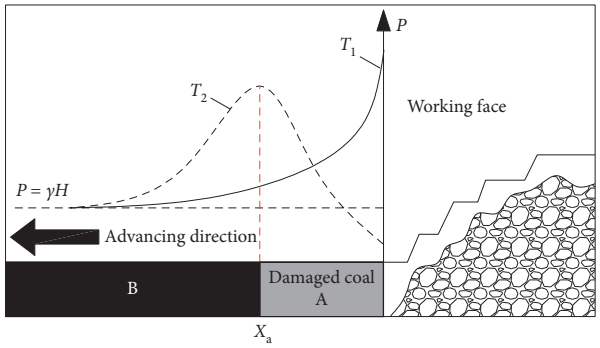

Figure 4: Schematic diagram of mining.

stress of coal particles on both sides of a certain interface share the same direction and magnitude.

(3) The wave form of the vibration load σ^* on the coal wall in Area B is approximately rectangular, and the duration of σ^* is t_1.

(4) The average yield stress of postpeak strain softening coal in Area B is Y_H.

(5) The elastic-plastic interface in front of the working face is X_a, and the densities of plastic and elastic coals are both ρ_0.

(6) The compressive stress is positive, while the tensile stress is negative.

The wave impedances of coal on both sides of the elastic-plastic interface in front of working face are not equal, and the wave impedance $\rho_0 c_1$ of plastic coal is smaller than the wave impedance $\rho_0 c_e$ of elastic coal. Because of these facts, during vibration loading, the loading and unloading stress waves will be transmitted and reflected when propagating to the interface. Moreover, compared with the incident wave, the transmitted and reflected waves are subjected to strengthened loading and unloading effects. The propagation and action process of loading and unloading stress waves in coal is shown in Figure 5.

From Figure 5, it can be observed that Zone 1 and Zone 1-1 are static zones (unaffected zones) where the stress and velocity of coal particles are

$$\begin{aligned} \sigma_1 &= \sigma_1' = 0, \\ v_1 &= v_1' = 0. \end{aligned} \tag{1}$$

When $t = t_0$, the coal is subjected to the action of vibration load σ^* (compressive stress), and the duration of σ^* is t_1. Accordingly, Zone 2 is the plastic loading zone where the stress and velocity of coal particles are

$$\begin{aligned} \sigma_2 &= \sigma^*, \\ v_2 &= -\frac{\sigma^*}{\rho_0 c_1}. \end{aligned} \tag{2}$$

When the plastic loading stress wave propagates to the interface X_a, transmission and reflection will occur. The stress and velocity of coal particles in Zone 3 are

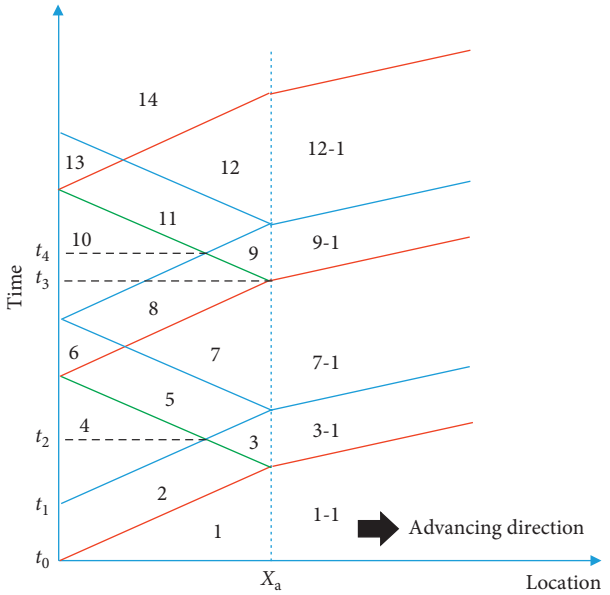

Stress wave propagation and action process

Figure 5: Stress wave propagation and action process in elasto-plastic coal.

$$\begin{aligned} \sigma_3 - \sigma_2 &= -\rho_0 c_1 (v_3 - v_1), \\ \sigma_4 &= 0. \end{aligned} \tag{3}$$

When $t = t_1$, the coal wall in Area B starts to unload, and the compressive stress in the coal instantly drops to zero. At this point, Zone 4 is a plastic unloading zone where the stress and velocity of coal particles are

$$\begin{aligned} \sigma_4 - \sigma_2 &= -\rho_0 c_1 (v_4 - v_2), \\ \sigma_4 &= 0, \\ v_4 &= 0. \end{aligned} \tag{4}$$

When $t = t_2$, the unloading wave from Zone 4 meets and interacts with the reflected unloading wave from Zone 3. At this time, the corresponding zone is Zone 5. In Zone 5, the tensile stress is superimposed, and the stress and velocity of coal particles are

$$\begin{aligned} \sigma_5 &= \frac{\sigma^* (c_e - c_1)}{c_1 + c_e}, \\ v_5 &= -\frac{\sigma^* (c_e - c_1)}{\rho_0 c_1 (c_1 + c_e)}. \end{aligned} \tag{5}$$

The stress and velocity of coal particles in Zone 6 are

$$\begin{aligned} \sigma_6 &= 0, \\ v_6 &= -\frac{2\sigma^* (c_e - c_1)}{\rho_0 c_1 (c_1 + c_e)}. \end{aligned} \tag{6}$$

When $t = t_3$, the unloading wave in Zone 10 meets and interacts with unloading wave in Zone 9 at the interface X_a, which further promotes the unloading effect of coal. At this

time, the corresponding zone is Zone 11 where the stress and velocity of coal particles are

$$\sigma_{11} = -\frac{\sigma^* (c_e - c_1)}{c_1 + c_e},$$
$$v_{11} = -\frac{\sigma^* (c_e - c_1)}{\rho_0 c_1 (c_1 + c_e)}. \quad (7)$$

When $t = t_4$, discharge and transmission will occur when the unloading wave in Zone 10 spreads to the interface X_a. At this point, the loading effect is relatively enhanced, forming a strengthened tensile stress wave. The corresponding zone is Zone 12 where the stress and velocity of coal particles are

$$\sigma_{12} = -\frac{2\sigma^* (c_e - c_1)}{(c_1 + c_e)^2},$$
$$v_{12} = \frac{2\sigma^* (c_e - c_1)}{\rho_0 c_1 (c_1 + c_e)}. \quad (8)$$

In summary, the analysis shows the following:

(1) During the propagation of the stress wave, tensile stress exists in Zones 8, 9, and 11, and compressive stress exists in Zones 2, 3, 5, and 14.

(2) During the propagation of the stress wave in the loading and unloading process, the tensile stress region and compressive stress region will appear circularly, and the stress and velocity of coal particles will gradually decrease by the multiple of $n_0 = (c_e - c_1)/(c_e + c_1)$. When the stress and velocity decay to approximately zero, the whole process of stress propagation is completed.

(3) The formation process of tensile stress is as follows: since the velocity c_l of the plastic wave is lower than the velocity c_e of the elastic wave, it can be obtained that the plastic unloading wave in Zone 6 meets and interacts with the plastic unloading wave in Zone 7. In Zone 8, the stress of coal particles changes to a positive value; that is, tensile stress is produced. When the right-lateral tensile stress wave in Zone 8 propagates to X_a, a strengthened tensile stress wave will be formed, leading to the increase of the tensile stress value.

At the same time, due to the weak capacity of the coal to bear tensile stress, the tensile stress existing in the coal tends to cause sharp damage to the coal. It can be seen that the unloading effect of coal plays an essential role in coal damage, and the coal undergoes tensile-shear failure under the combined action of tensile stress and in situ stress.

3.2. Theory of Dynamic Damage in Coal Wall. The coal in front of the working face includes plastic coal and elastic coal. In plastic coal, wave impedance increases with the increase of distance from the working face. If the plastic coal is divided into multiple regions, the wave impedances on both sides of the interface between two adjacent regions are not equal, and the wave impedance on the side closer to the coal wall is smaller than that on the side farther away from the coal wall. According to the propagation law of stress waves, vibration stress waves will be transmitted and reflected at the interface, resulting in strengthened loading and unloading waves in the coal.

In Figure 6, the disturbing stress waves generated by the operation of coal mining machinery can be divided into loading waves and unloading waves. When the stress waves are transmitted to the elastic-plastic interface, transmission and reflection will occur. When multiple unloading waves meet and superpose, the tensile stress zone may be formed. The tensile stress zone causes coal failure and a new elastic-plastic interface, which aggravates the failure. In contrast, when multiple loading waves meet and act on each other, stress concentration zones will be formed in the coal. As a result, the stress in the stress concentration area exceeds the ultimate strength of the coal and leads to the destruction of coal. The formation of a new destructive surface means the formation of a new reflection surface. As mentioned above, the reflection surface is more likely to produce tensile stress area and transform the stress concentration area in the coal into a tensile stress area. Due to the low tensile strength of coal, the damage occurs first in the tensile stress area. During the whole process of stress wave propagation, loading and unloading waves are constantly superimposed in the coal, gradually forming multiple stress concentration zones and tensile stress zones, which brings about the continuous production of new reflection surfaces. Meanwhile, the tensile stress zone is easy to be generated at the reflection surface so that the tensile stress zone continues to expand. Due to the existence of multiple stress concentration zones and tensile stress zones, the coal wall fails with various characteristics in different zones (i.e., experiences zonal failure) and undergoes spalling. Furthermore, the zonal failure gradually evolves into dynamic damage.

4. Discussion

In order to verify the above theory, a vibration experiment of coal samples was performed in this study. Cubic coal samples with a side length of 100 mm were prepared. In the experiment, the loading mode was displacement control; the displacement equation was the sine function with a frequency of 10 Hz and amplitudes of 0.5‰, 1‰, and 1.5‰, respectively. The experimental scheme is shown in Figure 7.

4.1. Stress-Strain Curve. Figure 8 illustrates typical curves obtained in the experiment. All of the curves have been subjected to three rates of loading. The loading path is from 0.5‰ to 1‰ and then to 0.5‰ in Figures 8(a) and 8(b), while it is from 0.5‰ to 1‰ and then to 1.5‰ in Figures 8(c) and 8(d).

As can be seen from Figure 8, the specific strain disturbance will cause loss of specific bearing capacity rather than failure of coal. In the same loading process, the bearing capacity of coal sample decreases gradually, with a trend of falling at an accelerated rate first and then declining steadily. In the experiment, when the strain disturbance changes from

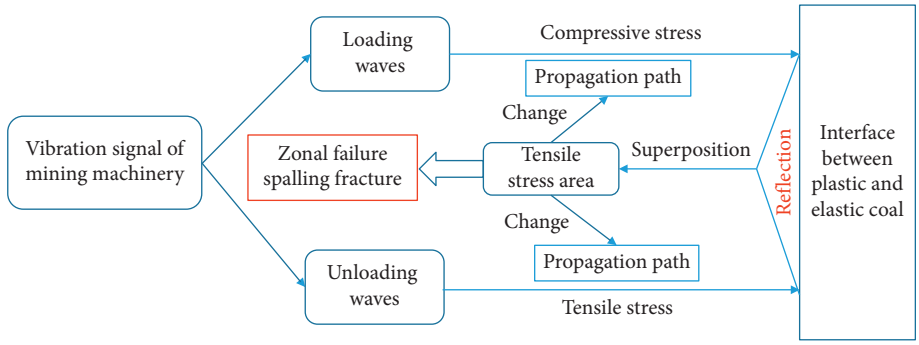

Figure 6: Theoretical model of coal wall dynamic damage.

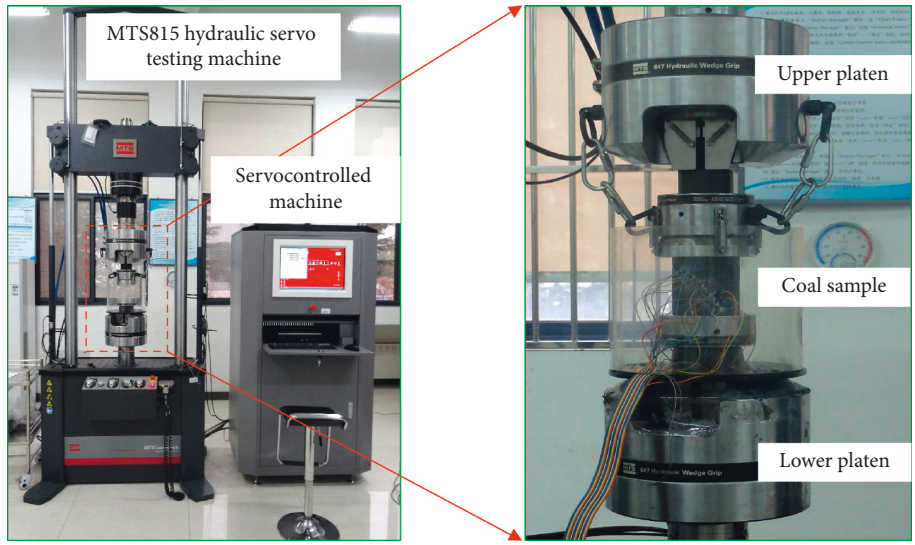

Figure 7: Vibration experiment of coal.

a small one to a large one, the bearing capacity of the coal sample will increase suddenly and the elastic modulus is pretty large. This is because when the loading rate rises suddenly, the internal structure of the coal sample fails to make a timely adjustment and thus becomes hardened to a certain extent. However, with the increase of disturbance strain, the range of bearing capacity reduction of samples also increases gradually, suggesting that large disturbance will cause great damage to coal. This finding is consistent with general knowledge. After a sample has undergone a large deformation disturbance, the small disturbance cannot further reduce its bearing capacity. Therefore, the bearing capacity remains at a certain level, and the sample possesses some residual strength. In conclusion, the sample gradually loses its bearing capacity under the action of disturbance load, presenting a dynamic failure process.

4.2. Failure Model. Figure 9 exhibits the failure modes of a coal sample. It can be seen from Figure 9 that the crack development of the coal sample is divided into five stages: integrity stage, transverse fracture propagation stage, mixed fracture propagation stage, longitudinal fracture propagation stage, and macrofracture coalescence stage.

The first stage is the integrity stage. During the 0–200 cycles of the experiment, there are no cracks on the surface of the sample, and the stress tends to be stable after decreasing. Stress is concentrated at the tip of original crack in the sample under the action of vibration load, and the crack loses the bearing capacity and closes gradually. As a result, the internal structure of the sample tends to be stable. The second stage is the transverse fracture propagation stage. During the 200–1000 cycles, transverse cracks appear on the surface of the sample, and the stress remains stable after a rapid decline. As shown by the theory of dynamic damage in coal, the vibration load and the reflected wave load are continuously superimposed in this stage. Nonuniform deformation emerges in the longitudinal direction of the sample, and tensile stress occurs at the part of the sample, which results in the generation of transverse cracks (equivalent to the deterioration of material properties). As a result, the bearing capacity of the sample is reduced, but the impact is limited. The third stage is the mixed fracture propagation stage. During the 1000–1100 cycles, the internal stress of the sample gradually decreases after a sudden increase. According to Poisson's ratio of coal, the transverse tensile stress of the sample exceeds the tensile strength, resulting in the generation of longitudinal cracks in the

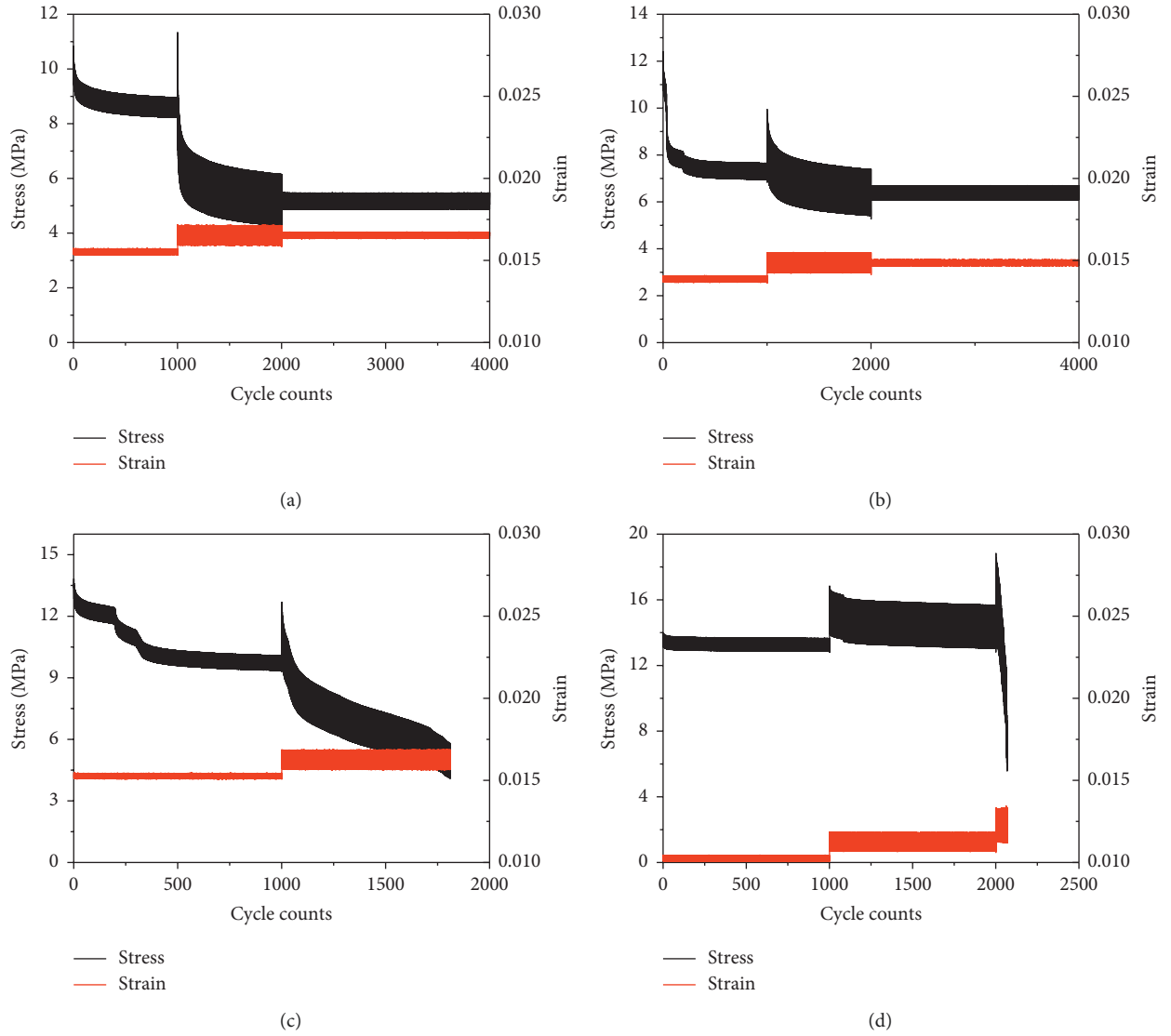

Figure 8: Diagram of stress-strain relationship under different loading paths. (a, b) Disturbance from 0.5‰ to 1‰ and then to 0.5‰. (c, d) Disturbance from 0.5‰ to 1‰ and then to 1.5‰.

sample. At the same time, the transverse cracks are generated under vibration load. In this way, the transverse cracks and the longitudinal cracks propagate together on the surface of the sample that demonstrates zonal failure. The fourth stage is the longitudinal fracture propagation stage. During the 1100–1600 cycles, more tiny coal particles slip on the surface of the sample under the vibration load, which further deteriorates the properties of the material. A longitudinal crack with a straight cross section appears in the sample which undergoes spalling. The fifth stage is the macrofracture coalescence stage. During the 1600–1800 cycles, the stress of the sample drops rapidly. As the damage of the sample develops to a certain extent, the sample can no longer bear the current stress load and gets destroyed rapidly, presenting a compressive-shear failure mode. Therefore, the crack growth is a gradual process, which is consistent with the theoretical explanation.

4.3. Dynamic Damage Evolution Process. Before the sample fails, microcracks are the main factor affecting the internal structure of the sample. The material properties deteriorate with the propagation of microcracks. Lemaitre [28] proposed the concept of continuous damage mechanics to simulate material damage. According to Lemaitre's strain equivalence hypothesis [29] and previous studies on damage under cyclic disturbance [30–32], the basic relationship of rock damage constitutive equation can be established as follows:

$$\sigma = E\varepsilon(1 - D), \tag{9}$$

where σ refers to the stress under each cyclic strain disturbance, E is the elastic modulus, D denotes the damage factor, and ε is the strain under each strain disturbance cycle.

By deforming the above formula, the damage factor can be expressed as

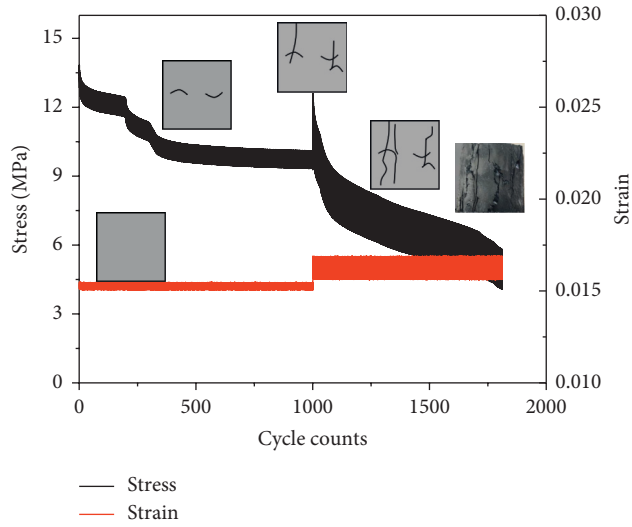

Figure 9: Failure mode of a coal sample.

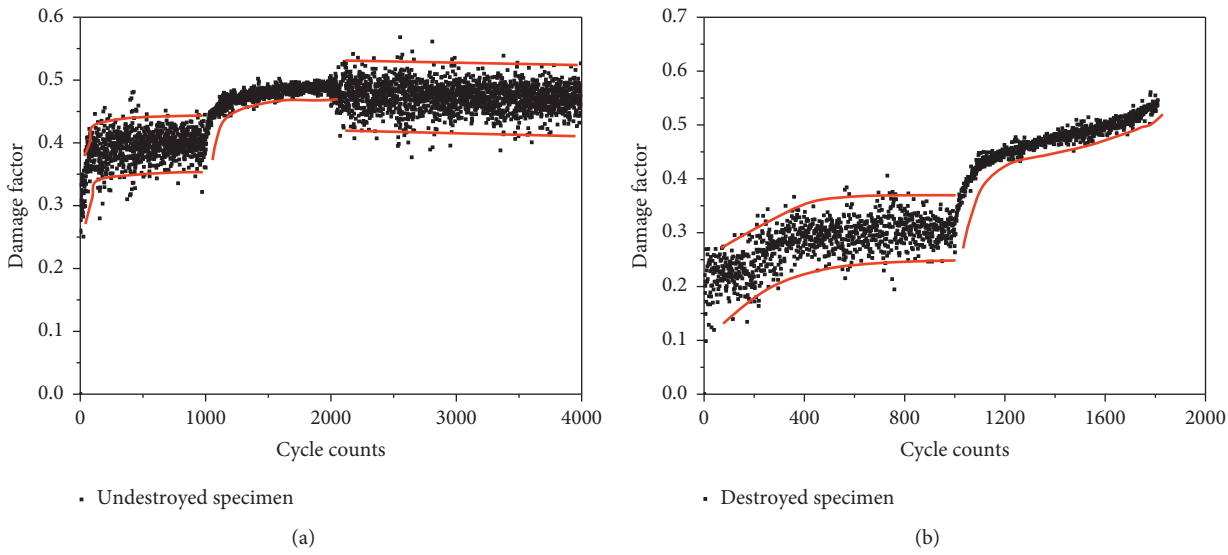

Figure 10: Relationship between the damage variable and the vibration number of the coal sample. (a) Disturbance from 0.5‰ to 1‰ and then to 0.5‰. (b) Disturbance from 0.5‰ to 1‰ and then to 1.5‰.

$$D = 1 - \frac{E'}{E}, \tag{10}$$

where E and E' denote the elastic moduli of undamaged and damaged materials, respectively. This paper assumes that the mesoscopic element and its damage are isotropic, so E, E', and D are all scalar.

In the process of coal sample failure under load, the current damage degree can be calculated according to the elastic modulus of the material. The elastic modulus of each vibration load is calculated according to equation (10). In this way, the relationship between the damage variable and the vibration number is obtained (Figure 10). Under the action of 0.5‰ strain disturbance, the damage factor of the sample tends to stabilize after increasing rapidly, indicating that the specific strain disturbance can only cause the damage in the sample to a certain extent. This is because the original microcracks in the sample are destroyed, which causes some irreversible deformation. However, after a certain number of vibrations, the sample no longer undergoes plastic deformation. When the strain disturbance grows to 1‰, the sample will be further damaged rapidly, after which the damage gradually stabilizes. However, if the material properties are further deteriorated, a large number of new cracks will appear. The damage factor will increase rapidly until the crack is formed and penetrated. After crack penetration, the bearing capacity of the sample is lost (Figure 10(b)). If the sample that has gone through a larger strain disturbance is treated with a smaller strain disturbance, the damage factor of the sample will remain stable without growing further (Figure 10(a)) because the small disturbance is not enough to satisfy the condition of internal

crack growth. Therefore, the process of sample failure is a dynamic damage process of internal crack compaction and closure and new crack generation and propagation under vibration disturbances [33].

5. Conclusions

In this paper, the vibration signals produced by the operation of mining machinery in coal were obtained, and the mechanism of vibration signals acting on coal was discussed. Besides, the mechanism of dynamic damage in coal wall was put forward and verified by an experiment. The main conclusions are as follows:

(1) By using the microseismic system, relatively pure-disturbance signals in coal wall were obtained for the first time. Disturbance signals exist in the form of the vibration wave, and their energy mainly is concentrated in two frequency bands, namely, 7–12 Hz and 12–27 Hz. The maximum displacement of the quadratic integral of vibration acceleration is 3.72 mm which can be regarded as a 1.2‰ strain disturbance.

(2) The law of stress wave propagation and action in coal wall was studied from the perspective of stress wave propagation. Moreover, based on the propagation and action of the vibration wave, the theory of dynamic damage in deep well working face was put forward.

(3) Under the influence of vibration disturbance, the crack development of a coal sample can be divided into five stages: integrity stage, transverse fracture propagation stage, mixed fracture propagation stage, longitudinal fracture propagation stage, and macrofracture coalescence stage.

(4) Based on the equivalent strain hypothesis, the process of damage factor evolution was investigated. Specific disturbance load will only cause a certain degree of damage to the sample. Greater disturbance can cause greater damage to the sample, and the specimen that has been subjected to greater load cannot be further damaged by smaller disturbance. Under the action of vibration load, the failure process is a dynamic process of crack compaction, closure, new crack formation, and propagation, which is verified by the damage statistical constitutive model established based on the isotropy hypothesis.

Data Availability

The data used to support the findings of this study are available from the corresponding author upon request.

Conflicts of Interest

The authors declare that there are no conflicts of interest regarding the publication of this paper.

Authors' Contributions

Shuaifeng Lu and Sifei Liu contributed equally to this work.

Acknowledgments

This research was funded by the "the Fundamental Research Funds for the Central Universities" (2018QNA24).

References

[1] B. Huang, H. Li, C. Liu, S. Xing, and W. Xue, "Rational cutting height for large cutting height fully mechanized top-coal caving," *Mining Science and Technology (China)*, vol. 21, no. 3, pp. 457–462, 2011.

[2] J. Kong, Q. S. Liu, Y. Q. Zhu, P. Chen, and H. An, "Research on comprehensive mechanized efficient construction technology of large section shaft in Hecaogou mine," *Advanced Materials Research*, vol. 753–755, pp. 853–856, 2013.

[3] J. H. Wang, "Key technology for fully-mechanized top coal caving with large mining height in extra-thick coal seam," *Journal of China Coal Society*, vol. 38, no. 12, pp. 67–70, 2013.

[4] Y. Yuan, S. H. Tu, and X. T. Ma, "Coal wall stability of fully mechanized working face with great mining height in "three soft" coal seam and its control technology," *Journal of Mining & Safety Engineering*, vol. 29, no. 1, pp. 21–25, 2012.

[5] Q. Yao, X. Li, B. Sun et al., "Numerical investigation of the effects of coal seam dip angle on coal wall stability," *International Journal of Rock Mechanics and Mining Sciences*, vol. 100, pp. 298–309, 2017.

[6] Y. Yuan, S. H. Tu, Q. Wu, M. Xiaotao, T. Hongsheng, and S. Lulu, "Mechanics of rib spalling of high coal walls under fully-mechanized mining," *Mining Science and Technology (China)*, vol. 21, no. 1, pp. 129–133, 2011.

[7] X. W. Yin, S. H. Yan, and Y. An, "Characters of the rib spalling in fully mechanized caving face with great mining height," *Journal of Mining & Safety Engineering*, vol. 25, no. 2, pp. 221–225, 2008.

[8] N. Yu, "Mechanism and control technique of the rib spalling in fully mechanized mining face with great mining height," *Journal of China Coal Society*, vol. 34, no. 1, pp. 50–52, 2009.

[9] G. F. Song, S. L. Yang, and Z. H. Wang, "Longwall face stability analysis using Ritz method and its 3D physical modelling study," *Journal of China Coal Society*, vol. 43, no. 8, pp. 2162–2172, 2018.

[10] J. C. Wang, "Mechanism of the rib spalling and the controlling in the very soft coal seam," *Journal of China Coal Society*, vol. 32, no. 8, pp. 785–788, 2007.

[11] L. M. Dou, X. Q. He, T. Ren et al., "Mechanism of coal-gas dynamic disasters caused by thesuperposition of static and dynamic loads and its control technology," *Journal of China University of Mining and Technology*, vol. 47, no. 1, pp. 48–59, 2018.

[12] L.-P. Cheng, C. Wang, L.-z. Tang et al., "Study on dynamic characteristics of deep siltstone under high static stress and frequent dynamic disturbance," *Advances in Civil Engineering*, vol. 2019, Article ID 2087684, 12 pages, 2019.

[13] S. You, H. Ji, Z. Zhang, and C. Zhang, "Damage evaluation for rock burst proneness of deep hard rock under triaxial cyclic loading," *Advances in Civil Engineering*, vol. 2018, Article ID 8193638, 7 pages, 2018.

[14] M. N. Bagde and V. Petroš, "Fatigue and dynamic energy behaviour of rock subjected to cyclical loading," *International Journal of Rock Mechanics and Mining Sciences*, vol. 46, no. 1, pp. 200–209, 2009.

[15] A. Hargraves and R. W. Upfold, "Aspects of laboratory simulations of instantaneous outbursts," in *Proceedings of the*

21st International Conference of Safety in Mines Research Institutes, pp. 129–137, Sydney, Australia, 1985.

[16] B. Li, Q. Zou, and Y. Liang, "Experimental research into the evolution of permeability in a broken coal mass under cyclic loading and unloading conditions," *Applied Sciences-Basel*, vol. 9, no. 4, 2019.

[17] J. Litwiniszyn, "A model for the initiation of coal-gas outbursts," *International Journal of Rock Mechanics and Mining Sciences & Geomechanics Abstracts*, vol. 22, no. 1, pp. 39–46, 1985.

[18] Y. Pan, G. Du, and Y. Zhang, "An experimental study on the mechanical properties of coal mass after vibrating," *Chinese Journal of Geotechnical Engineering*, vol. 20, no. 5, pp. 41–43, 1998.

[19] Z. Zhan and S. Qi, "Numerical study on dynamic response of a horizontal layered-structure rock slope under a normally incident SV wave," *Applied Sciences-Basel*, vol. 7, no. 7, 2017.

[20] J. Li and G. Ma, "Analysis of blast wave interaction with a rock joint," *Rock Mechanics and Rock Engineering*, vol. 43, no. 6, pp. 777–787, 2010.

[21] J. He, L.-M. Dou, W. Cai, Z.-L. Li, and Y.-L. Ding, "In situ test study of characteristics of coal mining dynamic load," *Shock and Vibration*, vol. 2015, Article ID 121053, 8 pages, 2015.

[22] F. Li, Y. G. Zhang, L. J. Rong et al., "Dynamic response characteristics of tectonic coal under dynamic loading," *Rock and Soil Mechanics*, vol. 36, no. 9, pp. 2523–2531, 2015.

[23] F. Li, M. Bi, F. Zhang et al., "Dynamic response characteristics and damage mechanisms of coal-rock masses under P-waves," *Journal of China Coal Society*, vol. 43, no. 5, pp. 1272–1280, 2018.

[24] X. Y. Sun, *The Research on Failure Characteristics and Disaster-Causing Mechanism of the Loaded Coal in Vibration*, China University of Mining & Technology, Beijing, China, 2016.

[25] C.-w. Li, C. Wang, B.-j. Xie, X.-y. Sun, and X.-m. Xu, "Study on low-frequency TEM effect of coal during dynamic rupture," *Shock and Vibration*, vol. 2015, Article ID 189569, 8 pages, 2015.

[26] X. Li, Z. Li, E. Wang et al., "Extraction of microseismic waveforms characteristics prior to rock burst using Hilbert-Huang transform," *Measurement*, vol. 91, pp. 101–113, 2016.

[27] J. Zhang, W. Peng, F. Liu, H. Zhang, and Z. Li, "Monitoring rock failure processes using the hilbert-huang transform of acoustic emission signals," *Rock Mechanics and Rock Engineering*, vol. 49, no. 2, pp. 427–442, 2016.

[28] J. Lemaitre, "A continuous damage mechanics model for ductile fracture," *Journal of Engineering Materials and Technology*, vol. 107, no. 1, pp. 83–89, 1985.

[29] J. Lemaitre, "How to use damage mechanics," *Nuclear Engineering and Design*, vol. 80, no. 2, pp. 233–245, 1984.

[30] X. S. Liu, J. G. Ning, Y. L. Tan, and Q. H. Gu, "Damage constitutive model based on energy dissipation for intact rock subjected to cyclic loading," *International Journal of Rock Mechanics and Mining Sciences*, vol. 85, pp. 27–32, 2016.

[31] X. Li, W.-G. Cao, and Y.-H. Su, "A statistical damage constitutive model for softening behavior of rocks," *Engineering Geology*, vol. 143-144, pp. 1–17, 2012.

[32] Z.-l. Wang, Y.-c. Li, and J. G. Wang, "A damage-softening statistical constitutive model considering rock residual strength," *Computers & Geosciences*, vol. 33, no. 1, pp. 1–9, 2007.

[33] Y.-J. Yang, L.-Y. Xing, H.-Q. Duan, L. Deng, and Y.-C. Xue, "Fatigue damage evolution of coal under cyclic loading," *Arabian Journal of Geosciences*, vol. 11, no. 18, p. 560, 2018.